Holon Wigner Crystal in a Lightly Doped Kagome Quantum Spin Liquid

Hong-Chen Jiang,[1,*] T. Devereaux,[1,†] and S. A. Kivelson[2,‡]
[1]Stanford Institute for Materials and Energy Sciences, SLAC and Stanford University, Menlo Park, California 94025, USA
[2]Department of Physics, Stanford University, Stanford, California 94305, USA
(Received 20 March 2017; published 7 August 2017)

We address the problem of a lightly doped spin liquid through a large-scale density-matrix renormalization group study of the t-J model on a kagome lattice with a small but nonzero concentration δ of doped holes. It is now widely accepted that the undoped ($\delta = 0$) spin-1/2 Heisenberg antiferromagnet has a spin-liquid ground state. Theoretical arguments have been presented that light doping of such a spin liquid could give rise to a high temperature superconductor or an exotic topological Fermi liquid metal. Instead, we infer that the doped holes form an insulating charge-density wave state with one doped hole per unit cell, i.e., a Wigner crystal. Spin correlations remain short ranged, as in the spin-liquid parent state, from which we infer that the state is a crystal of spinless holons, rather than of holes. Our results may be relevant to kagome lattice herbertsmithite upon doping.

DOI: 10.1103/PhysRevLett.119.067002

Introduction.—Broad interest in quantum spin liquid phases (QSLs) was triggered by the notion that they can be viewed as insulating phases with preexisting electron pairs, such that upon light doping they might automatically yield high temperature superconductivity [1–7]. It has also been proposed that a doped QSL might form an exotic topologically ordered Fermi liquid state (known as an FL* state) [8,9], or various other topologically ordered versions of familiar phases [10]. More broadly, it has been suggested that a host of behaviors of highly correlated electronic systems can be best understood from the perspective of doped spin liquids [11–16]. However, a "microscopic" theory of QSLs is difficult, as they seem to arise only in narrow portions of the generalized phase diagram where more typical broken symmetry states are suppressed by frustration, and in an "intermediate coupling" regime where neither the effective kinetic nor the interaction energy is dominant.

The spin-1/2 antiferromagnet on the kagome lattice (depicted in Fig. 1) with nearest-neighbor (NN) Heisenberg interactions, i.e., H_J in Eq. (1), is geometrically frustrated. A number of numerical simulations [17–22] have provided strong evidence that its ground state is a "Z_2-QSL" with exponentially falling spin-spin correlations and a nonzero spin gap, although some recent studies [23–28] have suggested that the true ground state may be a gapless (nodal) QSL. The fact that the observed spin correlation lengths in the earlier references are short compared to the width of the ladders studied leaves little room to doubt that they reflect the properties of a spin-gapped state. Nonetheless, it is plausible that there are at least two distinct QSL phases—one gapped and another ungapped—that are very close in energy such that the balance between them can shift as a function of ladder width, geometry, or slight changes in parameters; if this is the case it could reconcile the two sets of findings while leaving open the issue of which QSL is the ground state in the 2D limit.

Independent of which QSL has the lowest energy in two dimensions, in the present study, the fact that the spin correlation lengths we observe are several times shorter than the width of our cyllinders leaves little doubt that we are studying the properties of a doped, fully gapped Z_2 spin liquid. Experimentally, the celebrated material herbertsmithite is a realization of the two-dimensional kagome antiferromagnet [29,30], where the copper ions carry spin-1/2 magnetic moments which condense to form a QSL ground state. Specifically, experimental evidence of fractional spin excitations has been found in neutron scattering and strong indications of a spin gap are seen in NMR studies of single crystals [31,32].

The elementary excitations of a Z_2-QSL can be constructed [3,33] as combinations of a fermionic charge-0 spin-1/2 "spinon," a charge-e spin-0 bosonic holon, and a neutral topological "vison." The statistics of these particles is a matter of convenience—for instance, a fermionic holon can be constructed [34] as a bound state of a bosonic holon and a vison, while a normal spin-1/2, charge-e hole can be constructed as a bound state of a spinon and a holon. (We consider only hole doping of the QSL, so we can safely ignore negatively charged excitations.)

If we assume that the states achieved by adding a net positive charge density $\delta \ll 1$ per site to a QSL insulator can be described in terms of dilute excitations on top of a background QSL, then a variety of possible ground-state phases are natural to consider: If the lowest energy charged excitations are ordinary holes, then these can either remain itinerant, forming a FL*, (which is a distinct phase from a usual Fermi liquid as the Fermi surface only encloses an area corresponding to the density of doped holes, so

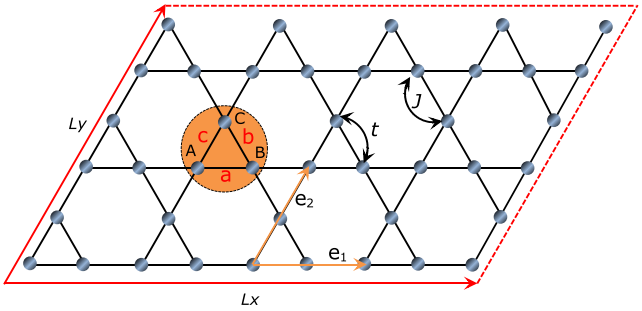

FIG. 1. The t-J model on a kagome cylinder, where the electrons live at the vertices (solid circles). Periodic (PBC) and open (OBC) boundary conditions are imposed, respectively, along the directions specified by the lattice basis vectors, e_2 and e_1. Each basis (denoted by small triangle in the shaded region) has three sites (A, B, and C) and three bonds (a,b, and c). t and J are hopping integral and spin exchange interactions between NN sites. L_x and L_y are the number of unit cells in the e_1 and e_2 directions.

violates Luttinger's theorem) or if they crystalize, they might form an insulating hole Wigner crystal (hWC) with one doped hole per emergent unit cell [35]. If, on the other hand, the lowest energy charged excitations are holons, then they could condense to form a conventional superconducting state with small superfluid density $\sim\delta$, or they could crystalize. We refer to the later state as WC*, which is distinguishable from hWC in that there are no low energy spin degrees of freedom. One could also imagine that the lowest energy charged excitations are holon pairs (or equivalently, spin-singlet hole pairs), which if they crystallize would form an insulating WC of Cooper pairs. Still more complicated phases could occur if a fraction of the charged excitations crystallize while others remain itinerant, or by condensing fermionic holons or bosonic spin-1/2 charge-e holes.

Principle results.—We find that the spin-spin correlation function (Fig. 2) is remarkably insensitive to doping. Indeed, the spin correlation length, $\xi_s \lesssim 2$ lattice constants, is small compared to the circumference of the cylinders studied and to the mean separation between doped holes. The fact that they look little different than those for $\delta = 0$ is consistent with viewing the system as a lightly doped QSL. The expectation value of the charge density (Figs. 4 and 5) is inhomogeneous, and the amplitude of the charge density variations is relatively insensitive to system size, implying that the ground state in the thermodynamic limit spontaneously breaks translation symmetry. Moreover, for the most part, the charge density appears to favor a triangular lattice with one doped hole per unit cell. Given the fact that there is no doping-induced magnetic order, we may identify this state as a WC*. However, the precise crystal structure of the WC* in the thermodynamic limit is not something we can infer with confidence, as in some cases, depending on the value of δ and the circumference of the cylinder, we find a stripe crystal rather than a triangular lattice. All superconducting correlations are extremely short-ranged (Fig. 3), with a correlation length $\xi_{SC} \lesssim 1.3$. [36]

Model Hamiltonian.—We employ the density-matrix renormalization group (DMRG) [38,39] to investigate the ground state properties of the hole-doped kagome t-J model depicted in Fig. 1 defined by the Hamiltonian

$$H = -t\sum_{\langle ij\rangle\sigma}(c^{\dagger}_{i\sigma}c_{j\sigma} + \text{H.c.}) + J\sum_{\langle ij\rangle}\left(\mathbf{S}_i\cdot\mathbf{S}_j - \frac{1}{4}n_i n_j\right), \quad (1)$$

where $c^{+}_{i\sigma}$ ($c_{i\sigma}$) is the electron creation (annihilation) operator with spin-σ on site i. $\vec{S}_i$ is the spin operator and $n_i = \sum_\sigma c^{+}_{i\sigma}c_{i\sigma}$ is the electron number operator. $\langle ij\rangle$ denotes NN sites and the Hilbert space is constrained by the no-double occupancy condition, $n_i \leq 1$. At half-filling, i.e., $n_i = 1$, the t-J model reduces to the spin-1/2 antiferromagnetic Heisenberg model.

The lattice geometry used in our simulations is depicted in Fig. 1, where $\mathbf{e}_1$ and $\mathbf{e}_2$ denote the two basis vectors. We consider kagome cylinders with periodic (open) boundary condition in the $\mathbf{e}_2$ ($\mathbf{e}_1$) direction. A cylinder geometry introduced Ref. [40] (which we will refer to as YC) is used such that one of the three bond orientations is along the $\mathbf{e}_2$ axis. Here, we focus on cylinders with width L_y and length L_x, where L_y and L_x are the numbers of unit cells ($2L_x$ and $2L_y$ are the number of sites) along the $\mathbf{e}_2$ and $\mathbf{e}_1$ directions, respectively. Notice that the unit cells at the right boundary of the cylinder contain only two sites (A and C) in order to reduce the boundary effects due to sharp edges. Following Refs. [18,40], we refer to the cylinders as YC-$2L_y$, whose total number of sites is $N = L_y(3L_x + 2) = N_u + 2L_y$, where N_u denotes the number of sites inside intact unit cells. In this Letter, we focus primarily on YC-6 and YC-8 cylinders, i.e., $L_y = 3$ and 4, with $L_x = 12$–24. We have also considered YC-10 cylinders, i.e., $L_y = 5$, and found similar results [see Fig. 4(e)]. As usual, the doping level of the system away from half-filling is defined as $\delta = N_h/N_u$, where N_h is the number of holes. Although $N_u \neq N$ so that the average value of δ differs slightly from $\tilde{\delta} = N_h/N$, deep in the bulk, i.e., relatively far from the open boundaries, $\tilde{\delta} = \delta$.

For the present study, we focus on the lightly doped case with $0 \leq \delta \leq 11\%$. We set $J = 1$ as an energy unit and consider $t = 3$. The results also hold for the other t. We perform up to 50 sweeps and keep up to $m = 10\,000$ DMRG states with a typical truncation error $\epsilon \sim 10^{-6}$ for YC-6 cylinders, $\epsilon \sim 10^{-5}$ for YC-8 cylinders, and $\epsilon \sim 5\times 10^{-5}$ for YC-10 cylinders. This leads to excellent convergence for our results when extrapolated to the $m = \infty$ limit (see the Supplemental Material [41].)

Spin-spin correlations.—To describe the magnetic properties of the ground state, we calculate the spin-spin correlation functions defined as $F(r) = (1/L_y)\sum_{y=1}^{L_y}|$

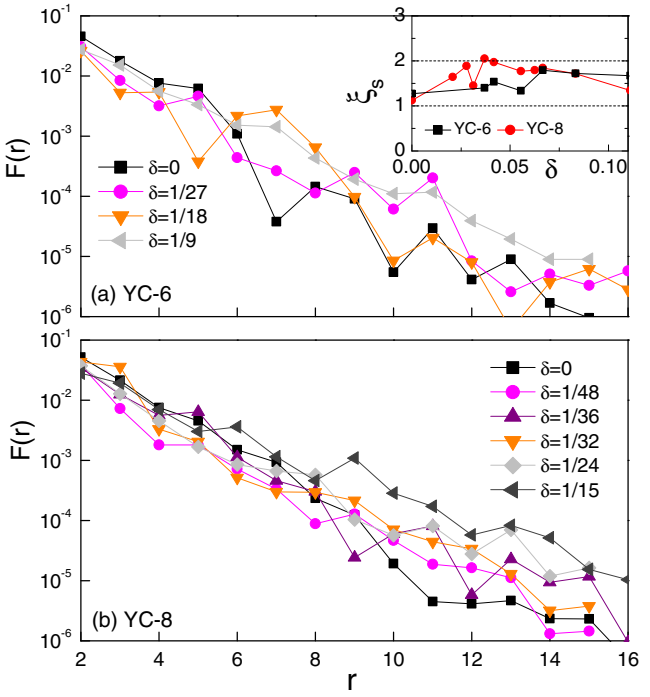

FIG. 2. The spin-spin correlation functions $F(r)$ along the $\mathbf{e}_1$ direction for (a) YC-6 and (b) YC-8 cylinders at different hole doping concentrations δ.r is the distance between two sites where the reference A site is in the middle of the system. Inset: The spin-spin correlation length ξ_s as a function of δ, by fitting $F(r)$ to an exponential function $F(r) \sim e^{-r/\xi_s}$. Here $L_x = 16$–24.

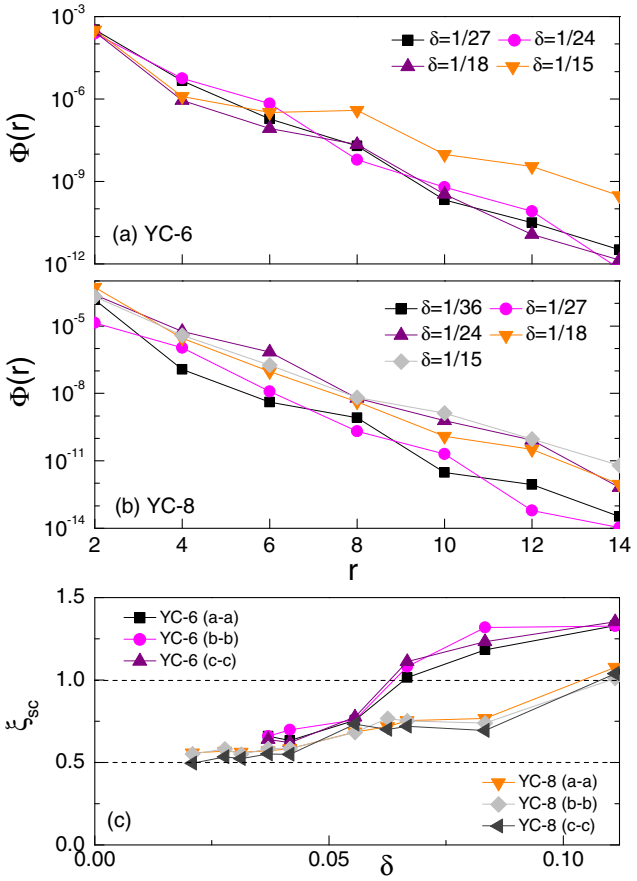

FIG. 3. The superconducting pair-field correlation functions $\Phi_{aa}(r)$ along the $\mathbf{e}_1$ direction between (a—a) bonds for (a) YC-6 and (b) YC-8 cylinders at different hole doping concentrations δ.r is the distance between two bonds with the reference bond in the middle of the system. (c) The superconducting correlation length ξ_{sc} as a function of δ, by fitting $\Phi(r)$ to an exponential function $\Phi(r) \sim e^{-r/\xi_{sc}}$. Here $L_x = 16$–24.

$\langle \mathbf{S}_0 \cdot \mathbf{S}_r \rangle|$. Here $\mathbf{S}_0$ denotes the spin operator on the reference A site in the middle of the cluster, while $\mathbf{S}_r$ runs over both A and B sites along the $\mathbf{e}_1$ direction with the distance r between them. At half-filling, i.e., $\delta = 0$, the ground state of the system is a QSL [17–20,40] with short-range spin-spin correlations. This is confirmed by our study where $F(r)$ for YC-6 and YC-8 cylinders in Fig. 2 both decay rapidly, and can be well fitted by an exponential function $F(r) \sim e^{-r/\xi_s}$ with short correlation lengths $\xi_s =$ 1.1–1.3 lattice spacings.

Upon doping, we find that the spin-spin correlations still remain short-ranged, where $F(r)$ for various $\delta > 0$ and different system sizes are shown in Fig. 2. For all cases, we find that $F(r)$ decays exponentially with small ξ_s, although ξ_s slightly depends on δ and lattice geometry. For both YC-6 and YC-8 cylinders, we find that $\xi_s = 1$–2 lattice spacings, similar to those of the QSL state of the undoped cylinder.

Superconducting correlation.—We have also investigated the possibility of superconductivity. Since the ground state remains a spin-singlet state upon doping, we focus on spin-singlet superconductivity. A diagnostic of superconducting order is the pair-field correlator defined as

$$\Phi_{\alpha\beta}(r) = \frac{1}{L_y} \sum_{y=1}^{L_y} |\langle \Delta_\alpha^\dagger(i_0) \Delta_\beta(i_0 + r) \rangle|. \quad (2)$$

Here, $\Delta_\alpha^\dagger(i)$ is the spin-singlet pair-field creation operator given by $\Delta_\alpha^\dagger(i) = (1/\sqrt{2})(c_{i\uparrow}^\dagger c_{i+\alpha\downarrow}^\dagger - c_{i\downarrow}^\dagger c_{i+\alpha\uparrow}^\dagger)$, where α denotes the bond type (see Fig. 1), i.e., a, b, or c, with bond vectors defined as $\mathbf{a} = \mathbf{e}_1/2$, $\mathbf{c} = \mathbf{e}_2/2$ and $\mathbf{b} = (\mathbf{e}_2 - \mathbf{e}_1)/2$. i_0 is the index of the reference bond in the middle of the cluster, and r is the distance between two bonds along the $\mathbf{e}_1$ direction.

In the present study, we find that Φ_{aa}, Φ_{bb}, Φ_{cc}, Φ_{ab}, Φ_{bc}, and Φ_{ca} all decay exponentially for both YC-6 and YC-8 cylinders [see Figs. 3(a) and 3(b)]. For large separations along the cylinder, $1 \ll |r| \ll L_x$, where $\mathbf{r} = r\hat{e}_1$, Φ can be well expressed as $\Phi_{\alpha\beta}(r) \sim e^{-|\mathbf{r}|/\xi_{\rm sc}^{\alpha\beta}}$ from which we derive the superconducting correlation length $\xi_{\rm SC}^{\alpha\beta}$. As shown in Fig. 3(c), $\xi_{\rm SC} = 0.5$–1.3 lattice spacings for all doping levels $0 < \delta \leq 11\%$ we have explored. Therefore, our results suggest that there is no (quasi-) long-range superconductivity in the doped kagome QSL.

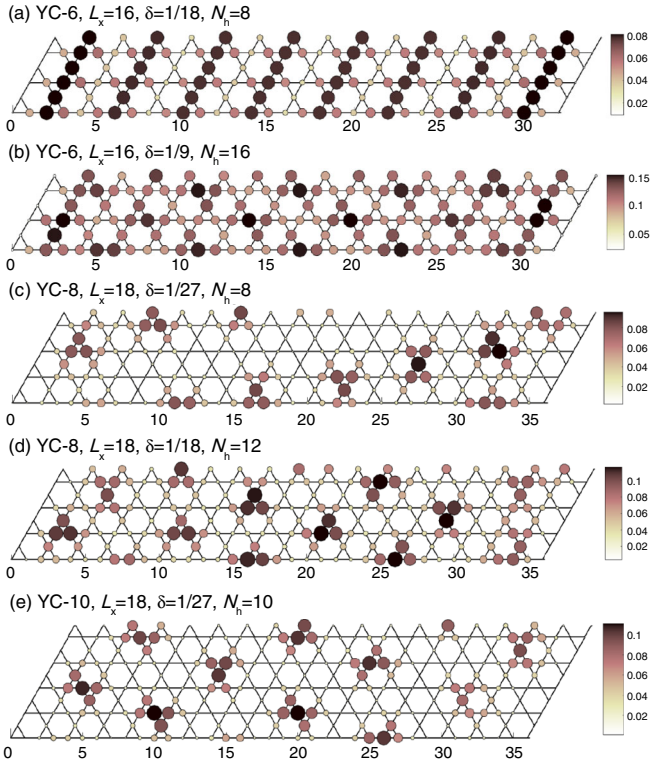

FIG. 4. The charge density profile $n_h(x, y)$ at different hole doping concentrations δ for YC-6 in (a)–(b), YC-8 in (c)–(d), and YC-10 cylinders in (e).

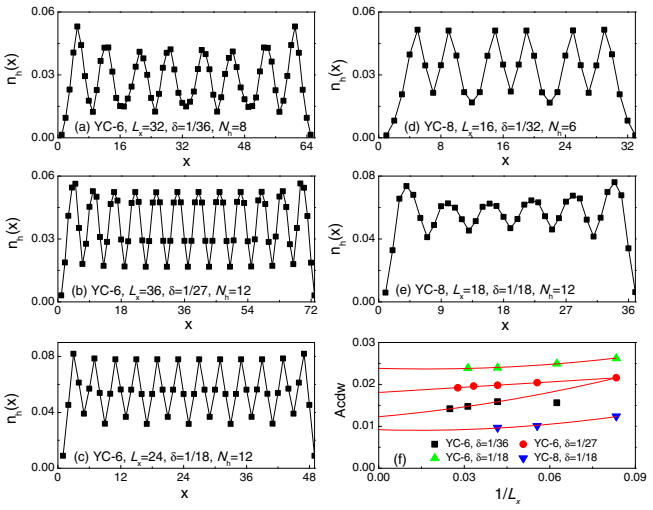

FIG. 5. The charge density profile $n_h(x)$ (includes both A and B sites) at different hole doping concentration δ for YC-6 in (a)–(c) and YC-8 cylinders in (d)–(e). (f) CDW order parameter A_{CDW} by fitting to $n_h(x)$ using function $n_h(x) = A_{\mathrm{CDW}} \cos(Q_{\mathrm{CDW}} x + \theta) + \cdots$, where Q_{CDW} is the ordering wave vector.

Charge density wave order.—Finally, we consider the charge density profile $n_h(x, y) = 1 - n(x, y)$, where $n(x, y)$ is the electron density on site $i = (x, y)$. Figure 4 shows some examples of $n_h(x, y)$ at different δ for YC-6, YC-8, and YC-10 cylinders. Clear CDW ordering is observed [42], although its pattern depends on both the lattice geometry and doping level. There is unidirectional CDW order at low doping levels for YC-6 cylinders, but this appears to be special for YC-6 geometry. For higher doping level for YC-6 cylinders and all doping levels for YC-8 cylinders, the CDW order resembles a two-dimensional Winger crystal, Figs. 4(b)–4(d).

Approximately, the doped system can be divided into new larger emergent unit cells, each containing one of the red stripes in Fig. 4(a) or one of the red spots in Figs. 4(b)–4(e); the number of emergent unit cells is equal to the number of doped holes at all doping levels. This is not a crystal of hole pairs.

To determine whether the CDW order survives in the thermodynamic limit, we further calculate the averaged rung charge density defined by $n_h(x) = (1/L_y) \sum_{y=1}^{L_y} n_h(x, y)$. Examples of $n_h(x)$ at different δ are plotted in Fig. 5. Here, the existence of long-range CDW order in the ground state can be determined by fitting the amplitude A_{CDW} of the oscillation of $n_h(x)$ and extrapolating the value to $L_x = \infty$. To minimize the boundary effect, we have removed four data points from both ends in the fitting process. Examples of the extrapolation are given in Fig. 5. The observed finite amplitude A_{CDW} in the thermodynamic limit establishes the presence of long-range CDW order.

Discussion.—In light of our observations, it is worth asking if there is an intuitive reason that the holons crystallize, rather than forming one of the possible quantum fluid states. It is already clear from previous numerical studies that the QSL in the kagome system is nearly degenerate with a number of possible valence-bond-crystalline phases. It is thus natural to imagine that the holon is a highly structured particle, surrounded by a "polaronic" cloud of valence-bond-crystal-like correlations.

In Fig. S3 in the Supplemental Material [41], we show that two doped holes in cylinders of moderate length ($L_x = 12$ and 16) induce a strong and extended pattern of valence-bond-crystalline order in their neighborhoods. The most obvious corollary is that the holon effective mass is strongly renormalized (increased). Moreover, the induced valence bond order implies the existence of moderate range effective interactions between holons, which if they are repulsive can naturally lead to crystallization. Note that in Fig. S2, we show that the spin gap with two doped holes (extrapolate to the $L_x \to \infty$ limit) is of the same order, although probably smaller than in the undoped ladder; this further corroborates our identification of this as a two-holon state.

Since the kagome antiferromagnet, i.e., H_J in Eq. (1), has been shown to be a realistic model to describe herbertsmithite [29,30], our results may be directly relevant to the real material upon doping. Consistent with our results, recent experimental studies have reported the

absence of superconductivity in kagome systems doped with either electrons [43] or holes [44]. While we have only studied finite cylinders, it is plausible that the results are representative of the thermodynamic limit, given the fact that the size of the cylinders, including both width L_y and length L_x, are much larger than both the spin-spin and superconducting correlation lengths.

We would like to thank Senthil Todadri, Young Lee, John Tranquada, Masaki Oshikawa, Arun Paramekanti, Roderich Moessner, Steve White, Zheng-Yu Weng, Hong Yao, and Shenxiu Liu and especially Leon Balents for insightful discussions, and John Dodaro for help making the figures. This work was supported by the Department of Energy, Office of Science, Basic Energy Sciences, Materials Sciences and Engineering Division, under Contract No. DE-AC02-76SF00515. Parts of the computing for this project were performed on the Sherlock cluster.

*hcjiang@stanford.edu
†tpd@stanford.edu
‡kivelson@stanford.edu

[1] P. W. Anderson, Science **235**, 1196 (1987).
[2] S. A. Kivelson, D. S. Rokhsar, and J. P. Sethna, Phys. Rev. B **35**, 8865 (1987).
[3] D. S. Rokhsar and S. A. Kivelson, Phys. Rev. Lett. **61**, 2376 (1988).
[4] R. B. Laughlin, Phys. Rev. Lett. **60**, 2677 (1988).
[5] X.-G. Wen and P. A. Lee, Phys. Rev. Lett. **76**, 503 (1996).
[6] L. Balents, Nature (London) **464**, 199 (2010).
[7] T. Senthil and P. A. Lee, Phys. Rev. B **71**, 174515 (2005).
[8] T. Senthil, S. Sachdev, and M. Vojta, Phys. Rev. Lett. **90**, 216403 (2003).
[9] M. Punk, A. Allais, and S. Sachdev, Proc. Natl. Acad. Sci. U.S.A. **112**, 9552 (2015).
[10] A. A. Patel, D. Chowdhury, A. Allais, and S. Sachdev, Phys. Rev. B **93**, 165139 (2016).
[11] P. A. Lee, N. Nagaosa, and X.-G. Wen, Rev. Mod. Phys. **78**, 17 (2006).
[12] A. Läuchli and D. Poilblanc, Phys. Rev. Lett. **92**, 236404 (2004).
[13] S. Guertler and H. Monien, Phys. Rev. B **84**, 174409 (2011).
[14] E. Fradkin, S. A. Kivelson, and J. M. Tranquada, Rev. Mod. Phys. **87**, 457 (2015).
[15] L. F. Tocchio, H. Lee, H. O. Jeschke, R. Valentí, and C. Gros, Phys. Rev. B **87**, 045111 (2013).
[16] E. Gull, O. Parcollet, and A. J. Millis, Phys. Rev. Lett. **110**, 216405 (2013).
[17] H. C. Jiang, Z. Y. Weng, and D. N. Sheng, Phys. Rev. Lett. **101**, 117203 (2008).
[18] S. Yan, D. Huse, and S. White, Science **332**, 1173 (2011).
[19] H. C. Jiang, Z. Wang, and L. Balents, Nat. Phys. **8**, 902 (2012).
[20] S. Depenbrock, I. P. McCulloch, and U. Schollwöck, Phys. Rev. Lett. **109**, 067201 (2012).
[21] S.-S. Gong, W. Zhu, L. Balents, and D. N. Sheng, Phys. Rev. B **91**, 075112 (2015).
[22] J.-W. Mei, J.-Y. Chen, H. He, and X.-G. Wen, Phys. Rev. B **95**, 235107 (2017).
[23] Y. Ran, M. Hermele, P. A. Lee, and X.-G. Wen, Phys. Rev. Lett. **98**, 117205 (2007).
[24] B. K. Clark, J. M. Kinder, E. Neuscamman, G. K.-L. Chan, and M. J. Lawler, Phys. Rev. Lett. **111**, 187205 (2013).
[25] Y. Iqbal, F. Becca, S. Sorella, and D. Poilblanc, Phys. Rev. B **87**, 060405 (2013).
[26] Y. Iqbal, D. Poilblanc, and F. Becca, Phys. Rev. B **89**, 020407 (2014).
[27] H. J. Liao, Z. Y. Xie, J. Chen, Z. Y. Liu, H. D. Xie, R. Z. Huang, B. Normand, and T. Xiang, Phys. Rev. Lett. **118**, 137202 (2017).
[28] Y.-C. He, M. P. Zaletel, M. Oshikawa, and F. Pollmann, arXiv:1611.06238.
[29] M. Hering and J. Reuther, Phys. Rev. B **95**, 054418 (2017).
[30] H. C. Jiang, J. Wen, and Y. S. Lee (to be published).
[31] T. H. Han, J. S. Helton, S. Chu, D. G. Nocera, J. A. Rodriguez-Rivera, C. Broholm, and Y. S. Lee, Nature (London) **132**, 5570 (2012).
[32] M. Fu, T. Imai, T.-H. Han, and Y. S. Lee, Science **350**, 655 (2015).
[33] T. Senthil and M. P. A. Fisher, J. Phys. A **34**, L119 (2001).
[34] S. Kivelson, Phys. Rev. B **39**, 259 (1989).
[35] Note that the hWC has a spin-$1/2$ per unit cell, and so would be expected to magnetically order unless the lattice structure of the hWC is such that this higher-order lattice supports a QSL ground state.
[36] It is worth noting that the phases of a putative doped QSL was considered in another recent DMRG study of the t-J model on the square lattice with a ratio of second and first neighbor exchange interactions, $J_2/J_1 \approx 1/2$ and with $\delta = 1/8$. While the systems considered there were much narrower than in the present study, clear evidence was found of a tendency to form a WC of singlet hole (or holon) pairs [37].
[37] J. F. Dodaro, H.-C. Jiang, and S. A. Kivelson, Phys. Rev. B **95**, 155116 (2017).
[38] S. R. White, Phys. Rev. Lett. **69**, 2863 (1992).
[39] H.-C. Jiang and L. Balents, arXiv:1309.7438.
[40] F. Kolley, S. Depenbrock, I. P. McCulloch, U. Schollwöck, and V. Alba, Phys. Rev. B **91**, 104418 (2015).
[41] See Supplemental Material at http://link.aps.org/supplemental/10.1103/PhysRevLett.119.067002 for more details.
[42] In the dilute doping limit, a phase separation instead of uniform charge-density-wave ordering is observed.
[43] Z. A. Kelly, M. J. Gallagher, and T. M. McQueen, Phys. Rev. X **6**, 041007 (2016).
[44] M.-H. Julien, V. Simonet, B. Canals, R. Ballou, A. K. Hassan, M. Affronte, V. O. Garlea, C. Darie, and P. Bordet, Phys. Rev. B **87**, 214423 (2013).